Atmos. Meas. Tech. Discuss., 4, 6969–6986, 2011
www.atmos-meas-tech-discuss.net/4/6969/2011/
doi:10.5194/amtd-4-6969-2011

Atmospheric Measurement Techniques Discussions

In situ study of particle growth in convective eddies of the planetary boundary layer

B. Alföldy[1], V. Groma[1], E. Börcsök[1], A. Nagy[2], A. Czitrovszky[2], and S. Török[1]

[1]Department of Health and Environmental Physics, Hungarian Academy of Sciences KFKI Atomic Energy Research Institute, P.O. Box 49, 1525, Budapest, Hungary
[2]Research Institute for Solid State Physics and Optics of the Hungarian Academy of Sciences, P.O. Box 49, 1525, Budapest, Hungary

Received: 28 September 2011 – Accepted: 17 October 2011 – Published: 23 November 2011

Correspondence to: B. Alföldy (alfi@aeki.kfki.hu)

Published by Copernicus Publications on behalf of the European Geosciences Union.

Abstract

A measurement flight was performed by a motorglider equipped with an aerosol size spectrometer and nano-particle counter over a large area in the rural vicinity of Budapest, Hungary. The flight was carried out in the early afternoon under unstable air dynamical conditions in August 2010. These conditions allowed flying in glider mode, with the engine switched off, using thermal lifts for altitude gain. A significant part of the flight was spent in thermals that allow studying how the atmospheric dynamics acts on the particle formation. It was found that hygroscopic growth affects the particle size distribution in the 30–500 nm interval. In the 30–280 nm interval, the growth rate was found to be similar to that of ammonium sulphate particles. Indirect signs of cloud droplet formation were found during cloud cross, as a concentration drop in size bins fallen in the 280–400 nm size range. In three thermal lifts significantly higher ultrafine particle concentration ($30 < d < 280$ nm) was measured, with decreased average diameter. The results support the supposition that convective eddies in the boundary layer affect the aerosol composition via hygroscopic growth and secondary particle formation.

1 Introduction

Aerosol is an inherent atmospheric component of which concentration is most difficult to couple to emission sources (in cases of measurement), or is predicted with the largest uncertainty (in cases of model calculation). This is the consequence of the wide set of sources (from natural to artificial) as well as the high complexity of physical and chemical processes that modify its concentration, physical properties, and chemical composition.

Secondary particle formation is probably the less known process of atmospheric aerosol production. Many experimental analyses and theoretical studies have investigated this phenomenon (Kulmala et al., 2004a; Holmes, 2007; Kulmala and Kerminen,

AMTD
4, 6969–6986, 2011

2008); however, none of them have provided a comprehensive description of the process. Consequently, contribution of secondary aerosols to the total aerosol budget is not fully yet clarified on both the meso- and macroscale.

It is known that secondary aerosol formation is a photochemistry related process (Kulmala and Kerminen, 2008). The physical-chemical processes that lead to the production of nanometer-size molecule clusters from gaseous vapours are studied in laboratory chamber experiments (Hu et al., 2007; Acker et al., 2006), and are modelled theoretically (Anttila et al., 2004; Kulmala et al., 2006). Particle formation takes place in a second step by the growth of the freshly nucleated clusters. What causes these clusters to grow is one of the most exciting open questions of aerosol science. Kulmala et al. (2004b, c) pointed to the condensation of organic vapours onto the surface of nanometer-size nuclei as the main process of the growth. This process needs well defined conditions and some kind of activation of the clusters before growth (Kulmala et al., 2006). It is currently debated what atmospheric conditions favour the nucleation and the subsequent growth. Easter and Peters (1994); Kerminen and Wexler (1995); Nilsson and Kulmala (1998); Khosrawi and Konopka (2003); and Lauros et al. (2006) have shown theoretically that turbulent motion of the air favours the nucleation. Antilla et al. (2004) suggested that nucleated clusters become activated in large eddies, resulting in new particle formation. From experimental studies Nilsson et al. (2001) reported that turbulent mixing triggers the particle formation events. Lauros et al. (2007) found correlation between the strength of the atmospheric mixing and new particle formation events. They concluded that vertical motion of air cell leads to higher saturation ratio of organic vapours due to the significant temperature drop that resulted by the adiabatic expansion of the air cell.

The basic goal of this work was to find experimental evidences for the link between secondary aerosol formation and atmospheric dynamics. For this purpose, airborne measurements were performed for mapping the horizontal as well as the vertical distribution of fine and ultrafine aerosol concentration in the planetary boundary layer.

AMTD
4, 6969–6986, 2011

Airborne investigations have a long history and high potential in the study of the atmosphere's composition. It was applied successfully in the last two decades for aerosol measurements involving detection of new particle formation (Baumgardner et al., 2011). Paris et al. (2009) published horizontal and vertical distribution of fine and ultrafine particles recorded during a large-scale aircraft observation in the Siberian free troposphere. They reported two cases of possible new particle formation in the upper troposphere and in an outflow of a convective cloud in the mid troposphere. Reeves et al. (2010), however, have published very low aerosol concentration in the fresh outflow of convective clouds, detected during measurement flights over the tropical region of West Africa. The authors explained their findings by wet removal of the aerosol via precipitation inside the convective cells. They also reported high nucleation mode particle concentration found over 8000 m. Recently, Junkermann et al. (2011) published their results on freshly nucleated and subsequently grown particles detected in the industrial/urban plume of Karlsruhe, Germany.

The scale of this work differs from the above mentioned examples. We have focused on the boundary layer of the atmosphere that requires low flying altitudes (below 2000 m) and low velocity for better spatial resolution. As a novel initiative, measurement flights were performed using a motorglider, without engine use, applying convective circulation for gaining altitude (thermal soaring). This flying style enables significant time spent in thermal lifts that permits the study of influence of convective circulation on the aerosol concentration and size distribution. Since the flight was coupled to the dynamics of the boundary layer, unique information was obtained about the relation of aerosol- and atmospheric-dynamics.

2 Instrumentation and measurement methods

Junkermann (2001) described an aerosol measurement setup installed on-board an ultralight aircraft. The system was capable of measuring aerosol size distribution in the

AMTD
4, 6969–6986, 2011

300 nm–20 µm diameter range, and the total particle number over 10 nm diameter. The system was applied in several campaigns (see e.g. the most recent; Emeis et al. 2011) and compared with other methodologies (Wiegner et al., 2006).

In this work a modified version of Junkermann's setup was used. The particle size distribution was recorded by a GRIMM 1.109 dust monitor in the 250 nm–30 µm diameter range, with 6 second time resolution. Later, one minute averages were generated and discussed. The size range is divided to 30 size bins. The cut-off diameters are 0.25, 0.28, 0.3, 0.35, 0.4, 0.45, 0.5, 0.58, 0.65, 0.7, 0.8, 1.0, 1.3, 1.6, 2.0, 2.5, 3.0, 3.5, 4.0, 5.0, 6.5, 7.5, 8.5, 10.0, 12.5, 15.0, 17.5, 20.0, 25.0, 30.0, 32.0 µm. Particles having diameters less than 250 nm are not detected by the instrument. The outlet of the instrument was connected to a GRIMM 1.320 NanoCheck particle counter that provides particle concentration in the 30–400 nm size range together with the average geometric particle diameter (this value is the average of the detected diameters weighted by their population, and generally differs from the mean diameter of the Aitken mode of the size distribution). The two instruments were integrated in a common housing provided by GRIMM Aerosol Technik GmbH, and the setup was previously calibrated by the company. The combination of the two instruments enables monitoring of the full aerosol size range from 30 nm up to 30 µm in different size channels. Air pressure, temperature and relative humidity were recorded by meteorological sensors. The position of the aircraft was registered by GPS.

The aerosol measurement system was fixed inside the cabin. The air sample was taken through a stainless steel inlet pipe bend mounted with a special tapered diffuser for ensuring isokinetic sampling condition. The pipe bend was transmitted through the cockpit canopy and connected to the inlet of the GRIMM 1.109 dust monitor by a 40 cm long antistatic plastic tube. Since flying without engine was planned during the measurement, the emission of the engine was not considered at the sampling installation. Data measured during engine use (at take-off and before landing) were ignored.

AMTD
4, 6969–6986, 2011

The aircraft measurement was performed on 11 August 2010 by an H-36 Dimona motorglider. The measurement flight started at 13:25 local time (11:25 UTC) from Dunakeszi airport that is a grassy sport airport 10 km north to Budapest (see Fig. 1). A 25 km × 25 km area was selected as a measurement sector in the north-east/east direction from Dunakeszi. In this zone the flying altitude is generally not limited; climbing is allowed up to the cloud base. Route of the measurement flight was about 140 km long (excluding spirals). The flying time was 3 h long, flying roughly within 2 h without engine.

At 13:50 the aircraft entered the measurement sector, and the engine was turned off. Afterwards the flight was performed in glider mode. In this flying mode aircraft continuously loses altitude in the surrounding air, and its vertical motion is connected to the uplift or descent of air masses. If the uplift of the surrounding air exceeds the descent of the aircraft – e.g. in a thermal lift – the aircraft gains altitude to the ground. When the pilot recognises the elevation change and takes the aircraft into a turn, it climbs along a spiral path (similarly to storks and hawks). At the top of the thermal the strength of the lift generally decreases. Reaching this altitude the pilot stops the spiralling and leaves the thermal. Accordingly, the path of the aircraft is a sequence of spiral uplifts (in the thermal lifts) and translations (between the lifts, see Fig. 1). In our case the shift of the aircraft was roughly vertical in thermal lifts (low wind velocity), while it was close to horizontal between the lifts (the average gliding angle calculated from the track log of the flight was roughly 4°–6° to the horizon). Since the aircraft continuously lost altitude during the translation, the pilot had to find thermal lifts for altitude retrieval. Presence of a thermal lift can be indicated by a cumulus cloud that is growing on the top of the thermal, or it can be concluded from the orography.

The advantage of this flight mode measurement comes from the force of altitude gaining that results in extended time spent in thermals. Altogether, 80 min were spent in thermals during the flight. Locations of thermals can be identified subsequently based on the track of the flight (spiral motion and altitude gain). This measurement mode can provide unique information about the air composition and meteorological

AMTD
4, 6969–6986, 2011

conditions in thermal lifts. The measured components can be compared in thermals and the intra-thermal regions, and the dynamical structure of the boundary layer can be studied.

3 Results and discussion

Variation of the total particle concentration in the 30–280 nm size range (referred to as ultrafine particles in the following) during the flight is presented in the upper panel of Fig. 2 together with the variation of the average particle diameter of the concerned size range. The ultrafine particle concentration was calculated as a difference of particle concentrations in the 30–400 nm size interval (measured by NanoCheck) and in the 280–400 nm range (measured by GRIMM 1.109). Since the difference of the particle population in the original and the narrowed size ranges is less than 1 %, the average diameter provided by NanoCheck can be accepted as a relevant value for the narrowed (30–280 nm) size range as well. All concentration data refer to standard conditions of 273 K and $P = 1013$ hPa.

Variation of flying altitude is shown in the lower panel of Fig. 2. It can be seen that the average diameter has high variability during the flight in accordance with the altitude variation. However, the number concentration has less variability in the concerned time interval (13:50–15:35) and this variability is not linked to the altitude change except for the three peaks marked in the figure that are discussed in the following.

At 13:55 the glider entered a thermal and the altitude started to increase. Three minutes later the particle concentration started to increase as well. In the next minutes the lift decreased and the glider left the thermal. The particle concentration increased for the next two minutes, then remained unchanged for 5 min. At 14:10 the concentration suddenly decreased and stabilized around 4000 counts per cm^3 level.

The next particle concentration peak started to form at 14:57 – a few minutes before the glider reached its maximal altitude in the concerned thermal. The particle concentration increased until 15:04, when the glider left the lift and shoved out by 6 km from

AMTD
4, 6969–6986, 2011

the thermal. During this increase of particle concentration a simultaneous decrease of the average diameter can be observed (from 93 nm to 70 nm). The third particle concentration peak started forming at 15:23 at the maximal elevation of the glider. Five minutes later the concentration reached its maximum and started to decrease. A simultaneous decrease of the average diameter accompanied the concentration increase, like in the previous case.

The simultaneous increase of concentration and decrease of average diameter of ultrafine particles reported above can be considered as an indirect sign of formation and/or growth of new particles. Since the minimal detectable particle diameter was 30 nm, pure nucleation events – which occurs in the few nm size range (Curtius, 2006) – could not be observed directly by our system. However, the tail of the size distribution of nucleation mode particles can exceed 30 nm (O'Halloran et al., 2009); consequently, nucleation events can be detected in the measurement range of our system. The concentration increase in the 30–280 nm size interval is equivalent with new particle appearance in the interval. The simultaneous decrease of the average diameter proves that new particles entered through the lower end of the interval.

Since particle counting in the lowest, 250–280 nm size bin of GRIMM 1.109 has high uncertainty, the next 280–300 nm bin was selected for further discussion. The upper panel of Fig. 3 shows variations of particle concentration in this size bin. Concentration values are shown in the left vertical axis. Particle mass concentration below 280 nm diameter (mass of ultrafine particles) is plotted in the figure as well, against the right axis. Particle mass values were calculated from particle number and average diameter measured by NanoCheck, assuming spherical shape and 1 g cm^{-1} density. In the lower panel of the figure particle number concentrations in the 350–400 nm and 450–500 nm size bins were plotted. As it can be deducted from the figures, particle concentrations and mass concentration follow more or less the altitude variation. This behaviour can be explained by hygroscopic growth of the particles: the higher the altitude, the higher the relative humidity that results hygroscopic particles growth. As a result from hygroscopic growth, particles having original diameters lower than the cut-off of the

AMTD
4, 6969–6986, 2011

size bin grow into the size bin and thus increase the particle population there. This phenomenon affects size bins up to 500 nm.

Hygroscopic growth of ultrafine particles can be studied directly in Fig. 4. Here the span of relative humidity change was divided into 15 intervals. Averages and standard deviations of each interval respecting both the relative humidity and average diameter of ultrafine particles were calculated and plotted in the figure. It can be seen that the average diameter of the ultrafine particle regime ($30 < d < 280$ nm) is a strictly increasing function of the relative humidity. The red line in the figure shows the theoretical curve for hygroscopic growth of ammonium sulphate particle with 50 nm dry diameter published by (Sjogren et al., 2007). The corresponding exponent of the power-law model of hygroscopic growth (Imre and Molnár, 2008) is 0.25. It can be seen that the growth factor for the ultrafine particles is similar to ammonium sulphate particles between 58 % and 91 % relative humidity ($d(91\,\%)/d(58\,\%)$); however, the measured data do not follow the power-law relation. This difference might be explained by the size dependency of the growth. It means that not only the mean diameter of the size distribution, but also the standard deviation increases during the growth.

The marked interval in Fig. 3 refers to a cloud cross event. At the top of the thermal, the glider reached the base of the cumulus cloud and entered in the cloud at 15:23. The glider spent 3 min in the cloud. In the cumulus cloud, reverse concentration variation can be observed in the ultrafine size range (see Fig. 2), and in the 280–300 nm and 350–400 nm size bins. The latter concentrations decreased, while ultrafine particle concentration increased. At the same time, average diameter of ultrafine particles dropped together with the calculated mass concentration.

This behaviour can be explained by an opposite aspect of particle growth. Loss of particles in the 280–300 nm and 350–400 nm size bins indicates that they grew out from the intervals. Over 450 nm cloud cross did not affect the particle concentration (see blue line in the lower panel of Fig. 3). The lost particles have not appeared in any of the upper size bins, what indicates that they grew over 10 µm and are deposited in the sampling line. Thus, the observed particle loss can be an indirect sign of cloud

AMTD
4, 6969–6986, 2011

droplet formation. It means that diameters of cloud nuclei extend up to 450 nm at 91 % relative humidity (directly prior to the cloud entrance).

The simultaneous concentration increase and diameter drop of ultrafine particles can be explained as an indirect sign of secondary particle formation and/or growth as it was discussed before.

4 Summary and conclusions

Chemical, physical modification of air pollutants, and atmospheric dynamics are related. A measurement platform has been installed on board a glider aircraft, providing unique information regarding the effect of atmospheric dynamics on particle formation and growth. As a new initiative, a research flight was performed in glider mode without engine use in order to follow the motion of the air parcel. Size fractioned particle concentration in the 250 nm–30 µm diameter range was measured with ultrafine particle concentration in the 30–400 nm size interval. Meteorological parameters such as air pressure, temperature, and relative humidity were also recorded.

The average diameter of the ultrafine particle regime was found to be correlated with relative humidity, indicating hygroscopic growth of the particles. The growth factor between 58 % and 91 % relative humidity was found to be similar to that of ammonium sulphate particles. Compared to the power-law model, a lower degree relationship was found between the average diameter and relative humidity, probably due to the size dependence of hygroscopicity. As a result of hygroscopic growth, mass variation of ultrafine particles followed the altitude variation. Particle concentration in the 280–500 nm size bin was also found to be correlated with flying altitude as another consequence of hygroscopic growth.

A decrease of particle concentration in the 280–450 nm diameter interval was found during cloud cross, indicating cloud droplet formation on cloud condensation nuclei.

An increase of ultrafine particle number concentration was observed in three thermals with a simultaneous drop of mean diameter. These events can be an indirect

AMTD
4, 6969–6986, 2011

indication of new particle formation/growth in convective eddies. This conclusion is confirmed by many theoretical as well as experimental studies (see Introduction), and supports the hypothesis that convective circulation is one of the most important sources of secondary formed aerosols.

Encouraged by the success of the simultaneous study of atmospheric dynamics and particle concentration by glider mode measurement method, further research flights are planned to be performed in different weather conditions. Particle detection threshold should be decreased down to ~5 nm to find direct evidences for the linkage of atmospheric dynamics and new particle formation.

Acknowledgements. Flight cost was covered by the Hungarian Meteorological Service. The GRIMM NanoCheck 1.320 portable nano-particle counter was submitted by the Grimm Aerosol Technik GmbH. Special thanks to our glider pilot, Géza Merka, whose contribution is highly appreciated.

References

Acker, K., Febo, A., Trick, S., Perrino, C., Bruno, P., Wiesen, P., Moller, D., Wieprecht, W., Auel, R., Giusto, M., Geyer, A., Platt, U., and Allegrini, I.: Nitrous acid in the urban area of Rome, Atmos. Environ., 40, 3123–3133, 2006.

Anttila, T., Kerminen, V.-M., Kulmala, M., Laaksonen, A., and O'Dowd, C. D.: Modelling the formation of organic particles in the atmosphere, Atmos. Chem. Phys., 4, 1071–1083, doi:10.5194/acp-4-1071-2004, 2004.

Baumgardner, D., Brenguier, J. L., Bucholtz, A., Coe, H., DeMott, P., Garrett, T. J., Gayet, J. F., Hermann, M., Heymsfield, A., Korolev, A., Kramer, M., Petzold, A., Strapp, W., Pilewskie, P., Taylor, J., Twohy, C., Wendisch, M., Bachalo, W., and Chuang, P.: Airborne instruments to measure atmospheric aerosol particles, clouds and radiation: A cook's tour of mature and emerging technology, Atmos. Res., 102, 10–29, doi:10.1016/j.atmosres.2011.06.021, 2011.

Curtius, J.: Nucleation of atmospheric aerosol particles, C. R. Physique 7, 1027–1045, 2006.

Easter, R. C. and Peters, L. K.: Binary homogeneous nucleation: temperature and relative humidity fluctuations, nonlinearity, and aspects of new particle production in the atmosphere, J. Appl. Meteorol., 33, 775–784, 1994.

AMTD
4, 6969–6986, 2011

Emeis, S., Forkel, R., Junkermann, W., Schäfer, K., Flentje, H., Gilge, S., Fricke, W., Wiegner, M., Freudenthaler, V., Groß, S., Ries, L., Meinhardt, F., Birmili, W., Münkel, C., Obleitner, F., and Suppan, P.: Measurement and simulation of the 16/17 April 2010 Eyjafjallajökull volcanic ash layer dispersion in the northern Alpine region, Atmos. Chem. Phys., 11, 2689–2701, doi:10.5194/acp-11-2689-2011, 2011.

Holmes, N. S.: A review of particle formation events and growth in the atmosphere in the various environments and discussion of mechanistic implications, Atmos. Environ., 41, 2183–2201, 2007.

Hu, D., Tolocka, M., Li, Q., and Kamens, R. M.: A kinetic mechanism for predicting secondary organic aerosol formation from toluene oxidation in the presence of NO_x and natural sunlight, Atmos. Environ., 41, 6478–6496, 2007.

Imre, K. and Molnár, A.: Hygroscopic behaviour of Central European atmospheric background aerosol particles in summer, Idojaras, 112, 63–82, 2008.

Junkermann, W.: An ultralight aircraft as platform, for research in the lower troposphere: system performance and first results from radiation transfer studies in straitform aerosol layers and broken cloud conditions, J. Atmos. Ocean. Tech., 18, 934–946, 2001.

Junkermann, W., Hagemann, R. and Vogel, B.: Nucleation in the Karlsruhe plume during the COPS/TRACKS-Lagrange experiment, Quartely Journal of the Meteorological Society, 137, 267-274, 2011.

Kerminen, V. M. and Wexler, A. S.: Growth laws for atmospheric aerosol particles: An examination of the bimodality of the accumulation mode, Atmos. Environ., 29, 3263–3275, 1995.

Khosrawi, F. and Konopka, P.: Enhanced particle formation and growth due to mixing processes in the tropopause region, Atmos. Environ., 37, 903–910, 2003.

Kulmala, M. and Kerminen, V. M.: On the formation and growth of atmospheric nanoparticles, Atmos. Res., 90, 132–150, 2008.

Kulmala, M., Vehkamäki, H., Petäjä, T., Dal Maso, M., Lauri, A., Kerminen, V. M., Birmili, W., and McMurry, P. H.: Formation and growth rates of ultrafine atmospheric particles: a review of observations, J. Aerosol Sci., 35, 143–176, 2004a.

Kulmala, M., Laakso, L., Lehtinen, K. E. J., Riipinen, I., Dal Maso, M., Anttila, T., Kerminen, V.-M., Hõrrak, U., Vana, M., and Tammet, H.: Initial steps of aerosol growth, Atmos. Chem. Phys., 4, 2553–2560, doi:10.5194/acp-4-2553-2004, 2004b.

Kulmala, M., Kerminen, V. M., Anttila, T., Laaksonen, A., and O'Dowd, C. D.: Organic aerosol formation via sulphate cluster activation, J. Geophys. Res., 109, 4205,

AMTD
4, 6969–6986, 2011

doi:10.1029/2003JD003961, 2004c.
Kulmala, M., Lehtinen, K. E. J., and Laaksonen, A.: Cluster activation theory as an explanation of the linear dependence between formation rate of 3nm particles and sulphuric acid concentration, Atmos. Chem. Phys., 6, 787–793, doi:10.5194/acp-6-787-2006, 2006.
Lauros, J., Nilsson, E. D., Vehkamäki, H., and Kulmala, M.: Atmospheric variability and binary homogeneous nucleation: A parametrisation and conditions required for a significant effect, Atmos. Res., 82, 503–513, 2006.
Lauros, J., Nilsson, E. D., Dal Maso, M., and Kulmala, M.: Contribution of mixing in the ABL to new particle formation based on observations, Atmos. Chem. Phys., 7, 4781–4792, doi:10.5194/acp-7-4781-2007, 2007.
Nilsson, E. D. and Kulmala, M.: The potential for atmospheric mixing processes to enhance the binary nucleation rate, J. Geophys. Res., 103, 1381–1389, 1998.
Nilsson, E. D., Rannik, U., Kulmala, M., Buzorius, G., and O'Downd, C. D.: Effects of continental boundary layer evolution, convection, turbulence and entrainment, on aerosol formation, Tellus, 53B, 441–461, 2001.
O'Halloran, T. L., Fuentes, J. D., Collins, D. R., Cleveland, M. J., and Keene, W. C.: Influence of air mass source region on nanoparticle events and hygroscopicity in central Virginia, US, Atmos. Environ., 43, 3586–3595, 2009.
Paris, J. D., Arshinov, M. Y., Ciais, P., Belan, B. D., and Nedelec, P.: Large-scale aircraft observations of ultra-fine and fine particle concentrations in the remote Siberian troposphere: New particle formation studies, Atmos. Environ., 43, 1302–1309, 2009.
Reeves, C. E., Formenti, P., Afif, C., Ancellet, G., Attié, J.-L., Bechara, J., Borbon, A., Cairo, F., Coe, H., Crumeyrolle, S., Fierli, F., Flamant, C., Gomes, L., Hamburger, T., Jambert, C., Law, K. S., Mari, C., Jones, R. L., Matsuki, A., Mead, M. I., Methven, J., Mills, G. P., Minikin, A., Murphy, J. G., Nielsen, J. K., Oram, D. E., Parker, D. J., Richter, A., Schlager, H., Schwarzenboeck, A., and Thouret, V.: Chemical and aerosol characterisation of the troposphere over West Africa during the monsoon period as part of AMMA, Atmos. Chem. Phys., 10, 7575–7601, doi:10.5194/acp-10-7575-2010, 2010.
Sjogren, S., Gysel, M., Weingartner, E., Baltensperger, U., Cubison, M. J., Coe, H., Zardini, A. A., Marcolli, C., Krieger, U. K., and Peter, T.: Hygroscopic growth and water uptake kinetics of two-phase aerosol particles consisting of ammonium sulphate, adipic and humic acid mixtures, J. Aerosol Sci., 38, 157–171, 2007.
Wiegner, M., Emeis, S., Freudenthaler, V., Heese, B., Junkermann, W., Munkel, C.,

AMTD
4, 6969–6986, 2011

Schafer, K., Seefeldner, M., and Vogt, S.: Mixing layer height over Munich, Germany: Variability and comparison of different methodologies, J. Geophys. Res., 111, D13201, doi:10.1029/2005JD006593, 2006.

AMTD
4, 6969–6986, 2011

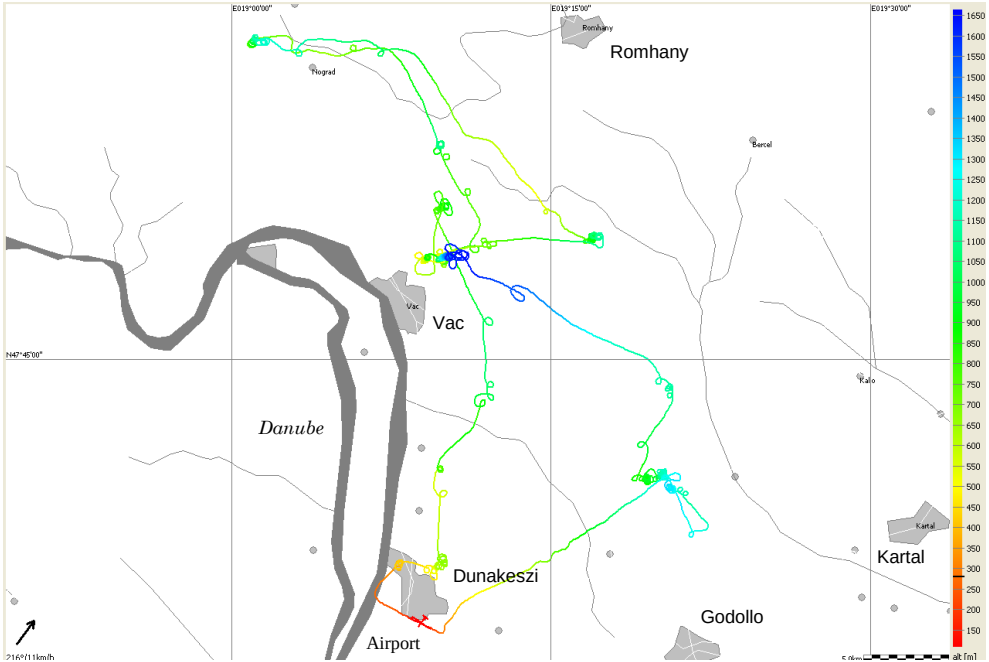

Fig. 1. Flying track on 11 August 2010. Colour code refers on the flying altitude over sea level.

AMTD
4, 6969–6986, 2011

In situ study of particle growth in convective eddies

B. Alföldy et al.

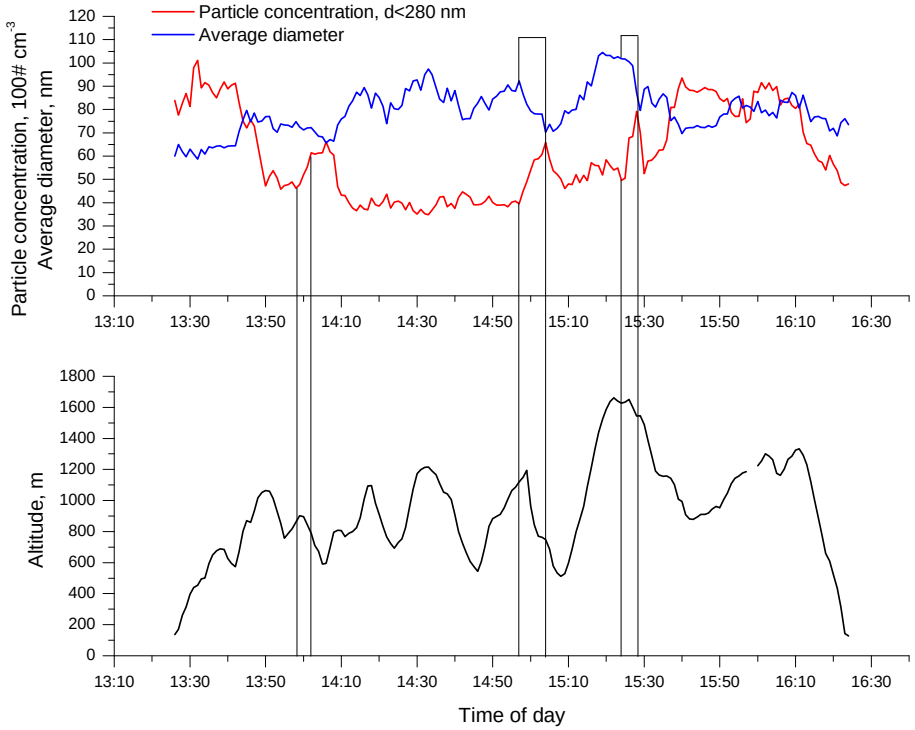

Fig. 2. Upper panel: variation of particle concentration and average diameter of the ultrafine particle range (30 nm < d < 280 nm). Lower panel: variation of flying altitude over sea level.

AMTD
4, 6969–6986, 2011

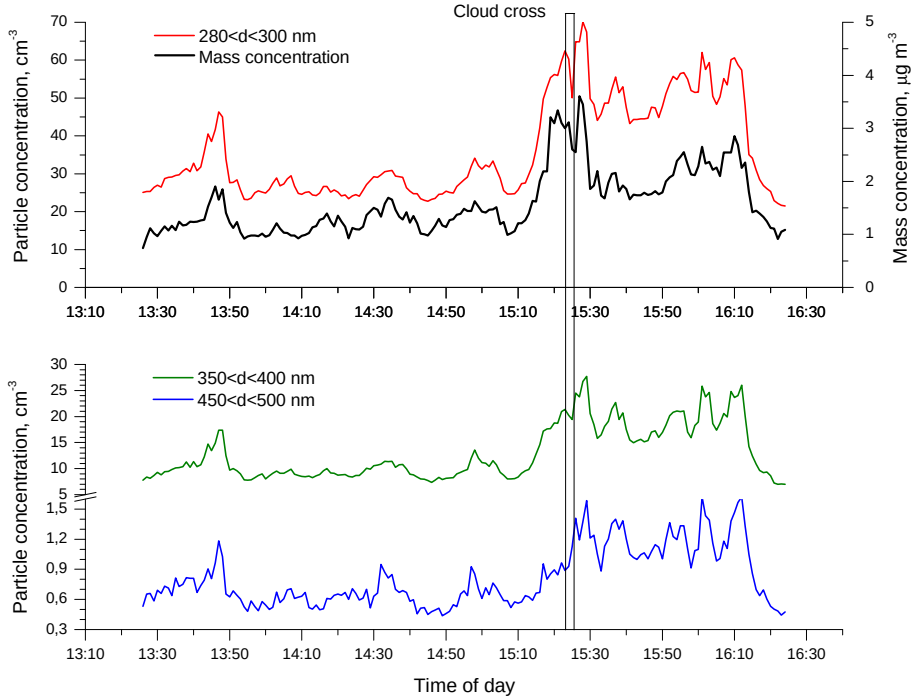

Fig. 3. Upper panel: variation of particle concentration in the 280–300 nm size interval, and particle mass in the ultrafine particle range. Lower panel: variation of particle concentration in the 350–400 nm and 450–500 nm size intervals.

AMTD
4, 6969–6986, 2011

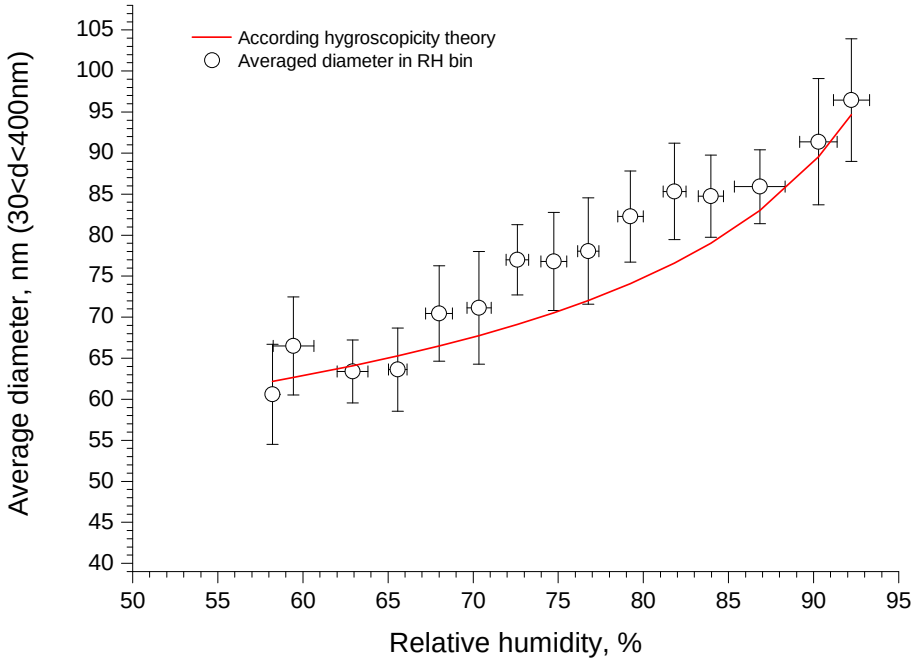

Fig. 4. Correlation between average diameter of the ultrafine particle size range and the relative humidity (dots). Solid line refers on hygroscopic growth of ammonium sulphate particles, with 50 nm dry diameter according to the power-law model of hygroscopicity.

AMTD
4, 6969–6986, 2011